3 FORWARD MODELING

3.1 Forward Modeling Method

Magnetic models of the subsurface sources for anomalies A, G, JF5, and Q were developed to better define the shape and nature of the sources. Magnetic intensity profiles, ground elevation values, and magnetometer boom elevations were extracted from the aeromagnetic databases using Oasis MONTAJ™ (Geosoft, 2006) and exported into GM-SYS© Version 4.8.45b (Northwest Geophysical Association, 2001) for the four two-dimensional modeled profiles developed for this report. Figure 3-1 replots the U.S. Department of Energy (DOE) helicopter aeromagnetic data and shows the areas covered by the two-dimensional forward models.

For each forward model, magnetic source bodies were developed as geologically reasonable polygons with known or inferred magnetic properties. Geometry of the source polygons was derived from a combination of known subsurface geologic conditions from the boreholes, extrapolation of nearby structures to the subsurface, analogs to similar features in the region, and general geologic principles. Source magnetic properties for each body were, at least initially, derived from published values or based on values for analogous rock types in the region. These were updated based on the magnetic data described in Section 2 of this report. Note that in the absence of measured declinations, declinations were assumed to be north for normal-polarity inclinations and south for reversed-polarity inclinations.

Forward modeling consisted of trial and error alteration of the polygons (both properties and geometries) until the models produced a magnetic response curve that closely matched the observed magnetic profile. Care was taken to preserve those aspects of the subsurface geometries that were known (e.g., depth to the top of the body based on borehole information) or were more likely to be known (e.g., projection of a nearby fault to the subsurface) and to alter only those aspects of the source geometry or magnetic parameters that were uncertain (e.g., lateral dimensions of the body in the subsurface or average remanent magnetization intensity). Forward models are nonunique solutions, and as shown by example in this report for anomaly A, the models evolved as more information became available. In particular, the results of the paleomagnetic and rock magnetic experiments constrained source parameters to known values and led to models that were more certain because they were better constrained by site-specific data.

3.2 Results of Forward Modeling

Anomaly A. Anomaly A has a distinct circular shape (Figure 3-2). The amplitude of anomaly A (peak to trough) at the elevation of the flight lines is more than 700 nT. It is located just south of Little Cone (Figure 3-1 and Figure 1-1), which restricts the placement of the profile for modeling the properties of the subsurface units. The profile for anomaly A was chosen such that it passed through the maximum amplitude of the anomaly and did not overlay the surface outcrop of Little Cone just north of the anomaly. As part of this study, before the paleomagnetic data listed in Table 2-9 were available, anomaly A was initially modeled as a series of faulted units of basalt flow, Ammonia Tank Tuff (Tma) and Rainier Mesa Tuff (Tmr), overlain on the top by Quaternary Alluvium (Qal) (Figure 3-3). In the initial model, the main basalt flow is normally magnetized (60°) with a strong remanent magnetization intensity (20 A/m). This initial

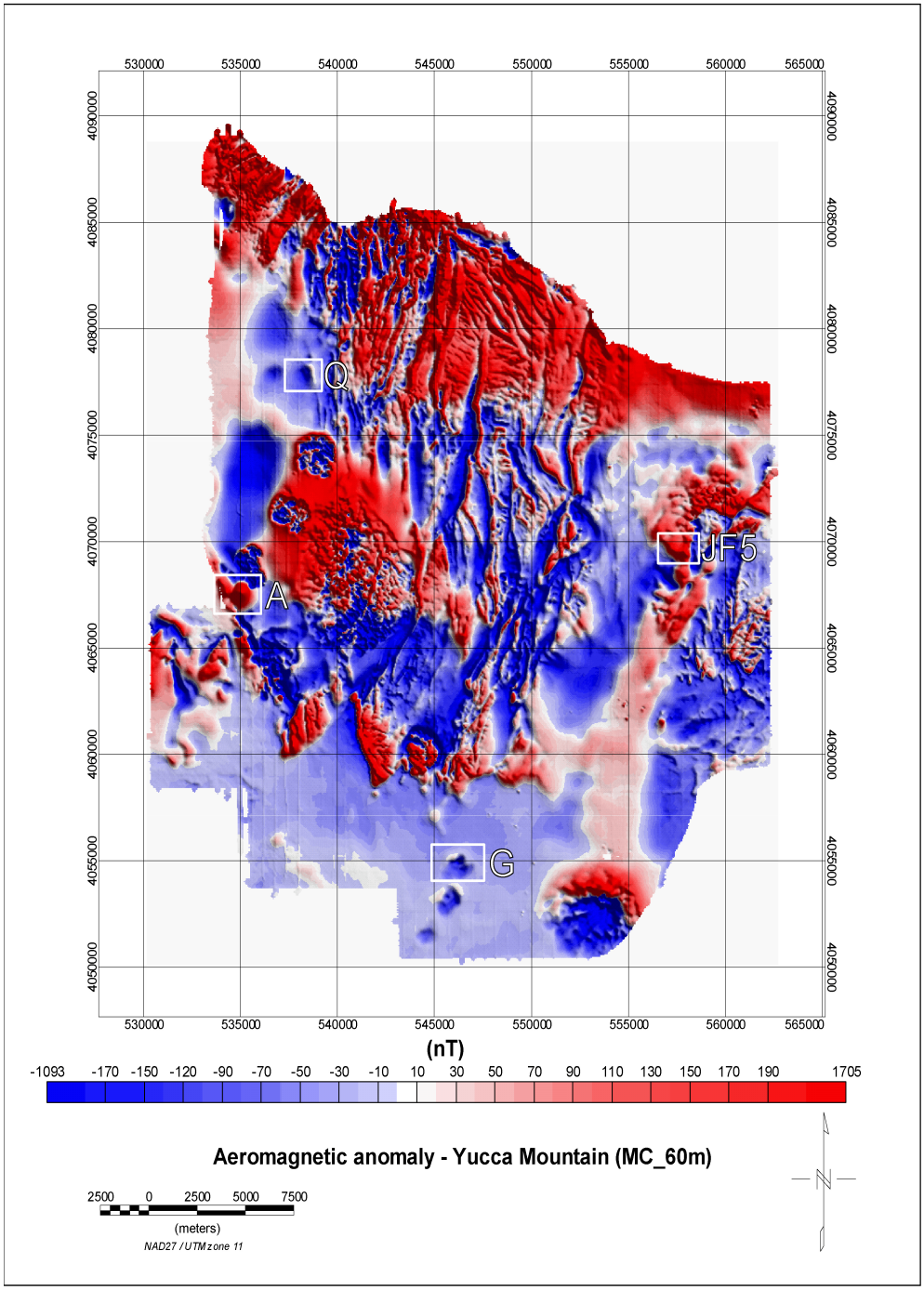

Figure 3-1. Total Field Aeromagnetic Anomaly Map Around Yucca Mountain, Nevada, Compiled at Approximately 30 m [98.42 ft] Above Ground Surface. The White Rectangles Show Anomalies A, G, JF5, and Q.

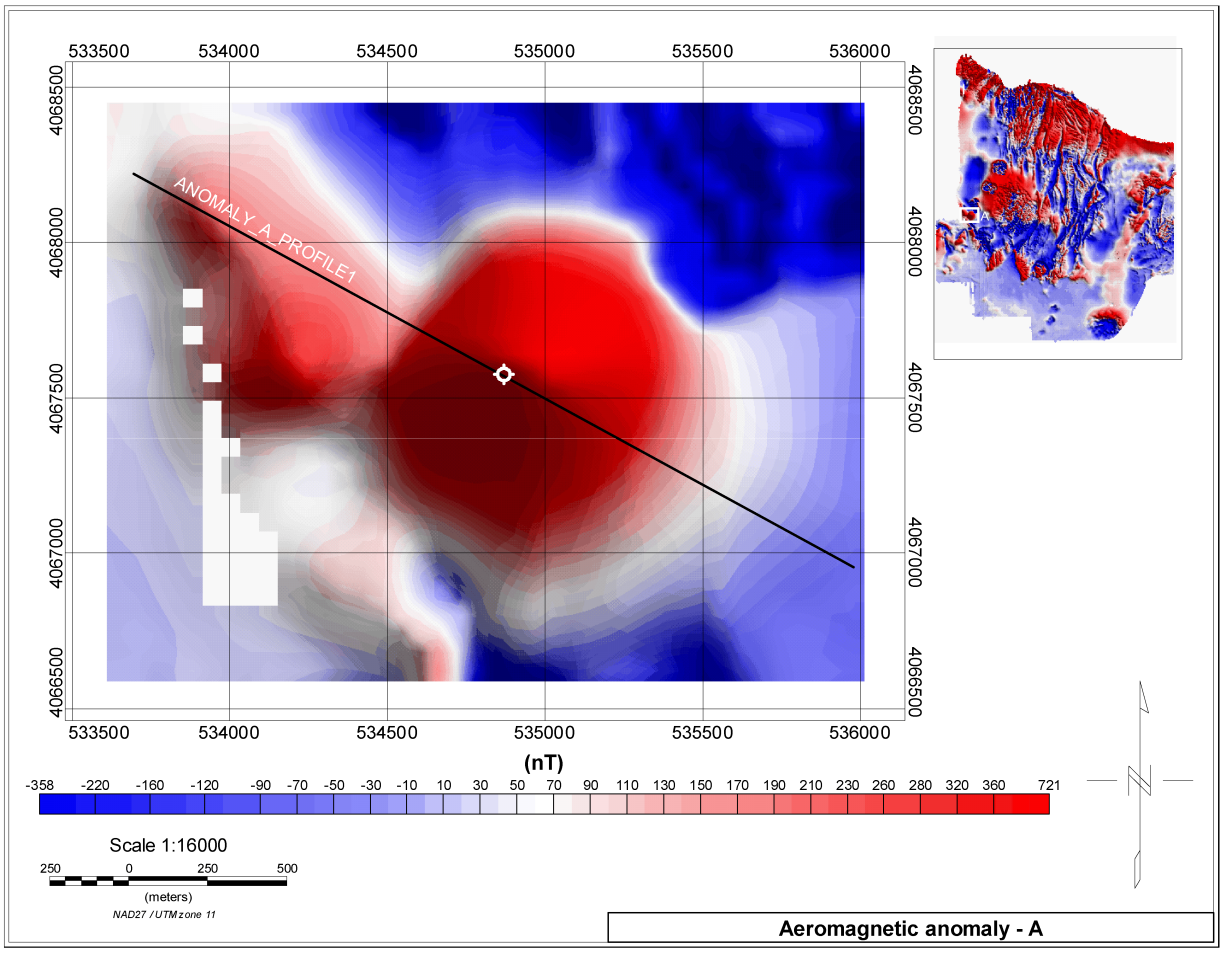

Figure 3-2. Total Field Aeromagnetic Anomaly A Showing Borehole Location and Profile Location for Two-Dimensional Modeling

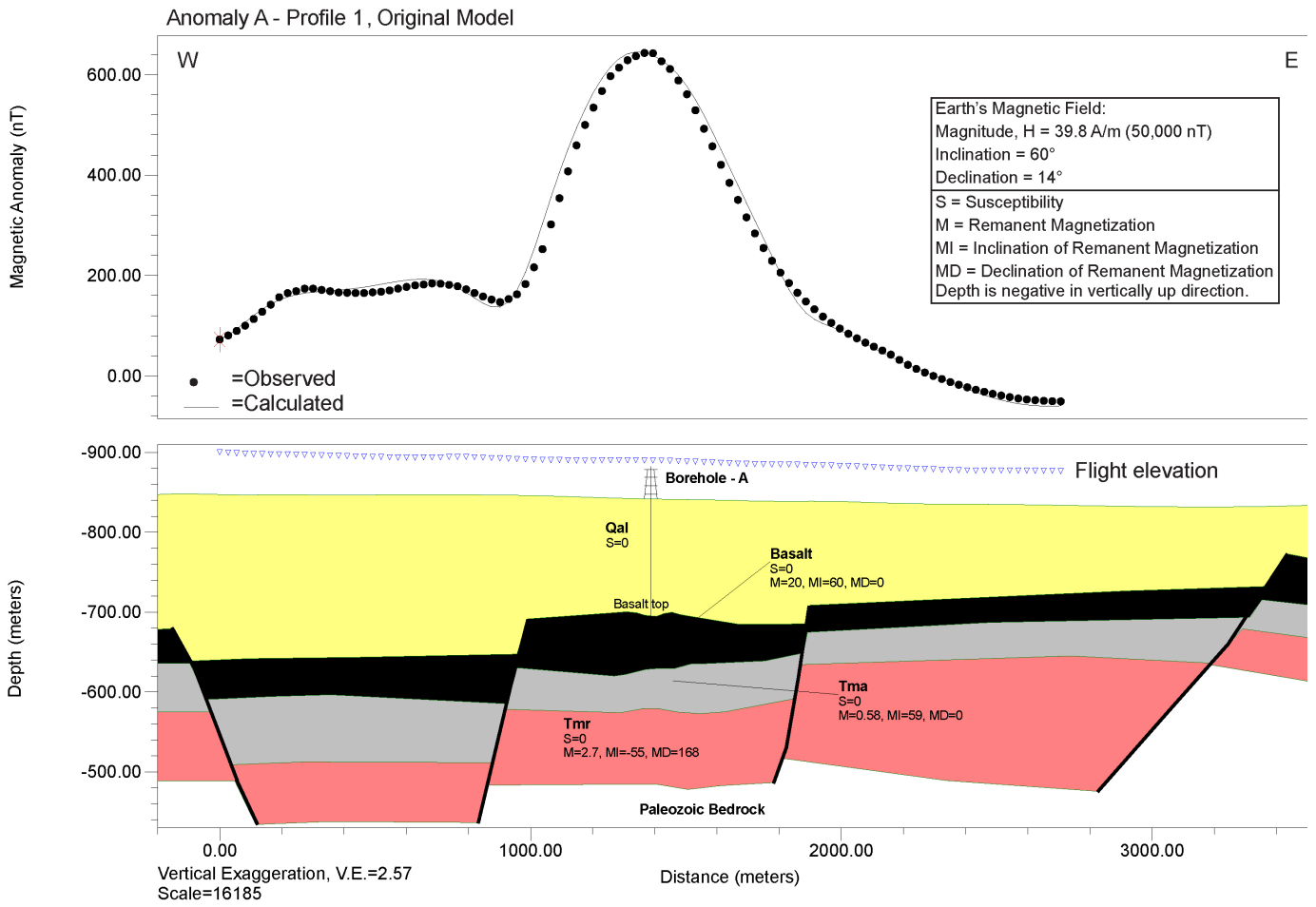

Figure 3-3. Original Two-Dimensional Model of Anomaly A Along Profile 1 Prior to Laboratory Measurements of Paleomagnetic Properties of Basalt Samples From Anomaly A Borehole. Qal–Quaternary Alluvium, Tma–Ammonia Tanks, Tmr–Rainier Mesa.

remanence was needed to match the observed anomaly to maintain the modeled flow layer structure. There are 11 Ma basalt outcrops immediately south to southeast of anomaly A, which supports the initial hypothesis of a thin stack of lavas. Similar remanence intensities were used to model basalt flows at Little Cone (Stamatakos, et al., 1997).

When, however, the laboratory measurements of the paleomagnetic properties (Table 2-9) of the basalt in anomaly A were applied to the initial model, it failed to match the observed anomaly (Figure 3-4). A lower measured magnetic intensity (2.46 A/m) for the basalt requires a much thicker body (Figure 3-5) compared to the faulted basalt flow in the previous scenario. The top of the basalt is constrained by the depth of basalt interception at the borehole location. To provide a sufficient magnetic source to match the observed 700 nT anomaly amplitude, a basalt >500 m [>1,640 ft] truncated by a fault has been modeled (Figure 3-5). A fault at this site is consistent with local geology [i.e., the Bare Mountain fault (Fridrich, 1999)]. The basalt is magnetized with a steep normal direction (59°). Such a thick source geometry is unlikely to be a series of lava flows or a buried volcanic cone. Instead it is consistent with an intrusion of magma into alluvium, such as a thick sill of an ancient volcanic conduit system.

Anomaly G. Anomaly G has a distinct dipolar pattern with high and low amplitudes, but the boundary between the high and low regions lacks any elongated trend (Figure 3-6). There are no surface exposures of igneous bodies around the anomaly to restrict the placement of the profiles. Two profiles were chosen for anomaly G such that they cover all the distinct features of the anomaly. Both profiles were modeled with a basalt flow of variable thickness buried in Quaternary Alluvium (Qal) (Figures 3-7 and 3-8). The top of the basalt is constrained by the depth of basalt interception at the borehole location. The maximum thickness of the basalt flow constrained by modeling is 80 m [262 ft].

Anomaly JF5. Anomaly JF5 shows a broad magnetic high in an east-west direction, and the boundary between the high and low pattern has a nearly north-south trend (Figure 3-9). The profile for anomaly JF5 was chosen such that it was approximately normal to the north-south trend and going through the maximum and minimum amplitude of the anomaly. The anomaly is modeled with a basalt flow of variable thickness buried in Quaternary Alluvium (Qal) and terminated by a normal fault on its east edge (Figure 3-10). The top of the basalt is constrained by the depth of basalt interception at the borehole location. The maximum thickness of the basalt flow constrained by modeling is 140 m [459 ft]. The modeled normal fault is a projection of the Gravity fault, which is inferred from other geophysical data to form the eastern boundary of Fortymile Wash (Potter, et al., 2002).

Anomaly Q. Anomaly Q has a distinct dipolar pattern with high and low amplitudes, and the boundary between the high and low pattern has a nearly north-south trend (Figure 3-11). The profile for anomaly Q was chosen such that it was oriented almost perpendicular to the north-south trend and going through the maximum and minimum in the amplitude of the anomaly. Anomaly Q was modeled as a series of faulted units of basalt flow, Ammonia Tank Tuff (Tma), and Rainier Mesa Tuff (Tmr), overlain on the top by Quaternary Alluvium (Qal) (Figure 3-12). The top of the basalt is constrained by the depth of basalt interception at the borehole location. The maximum thickness of the basalt flow constrained by modeling is 92 m [302 ft]. The basalt is magnetized with a shallow reverse inclination (−27°). The normal fault blocks are consistent with the inferred subsurface geology in the Crater Flat region (e.g., Fridrich, 1999).

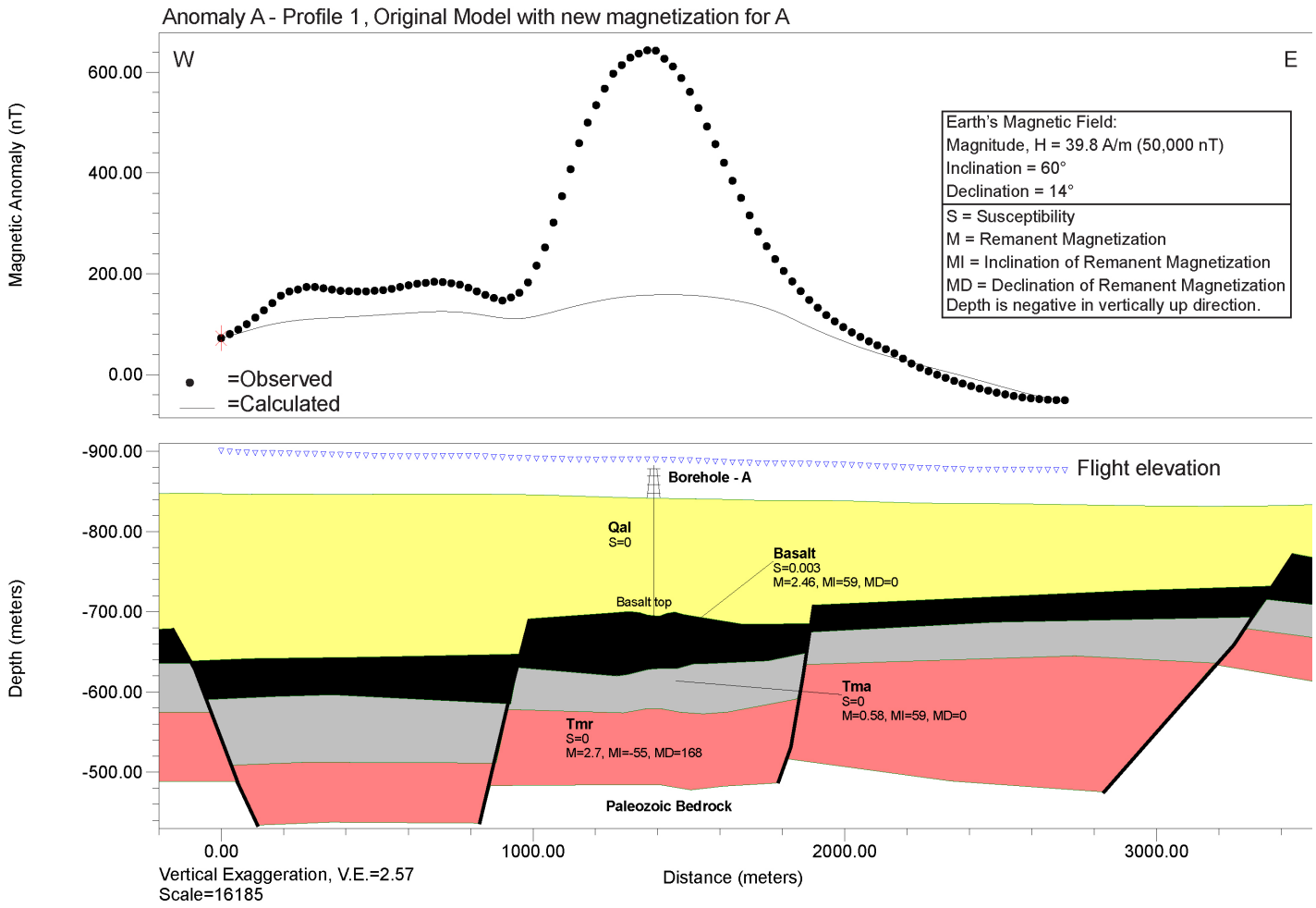

Figure 3-4. Original Two-Dimensional Model of Anomaly A Along Profile 1 With New Intensity of Basalt Showing the Misfit Between Observed and Calculated Anomaly. Qal–Quaternary Alluvium, Tma–Ammonia Tanks, Tmr–Rainier Mesa.

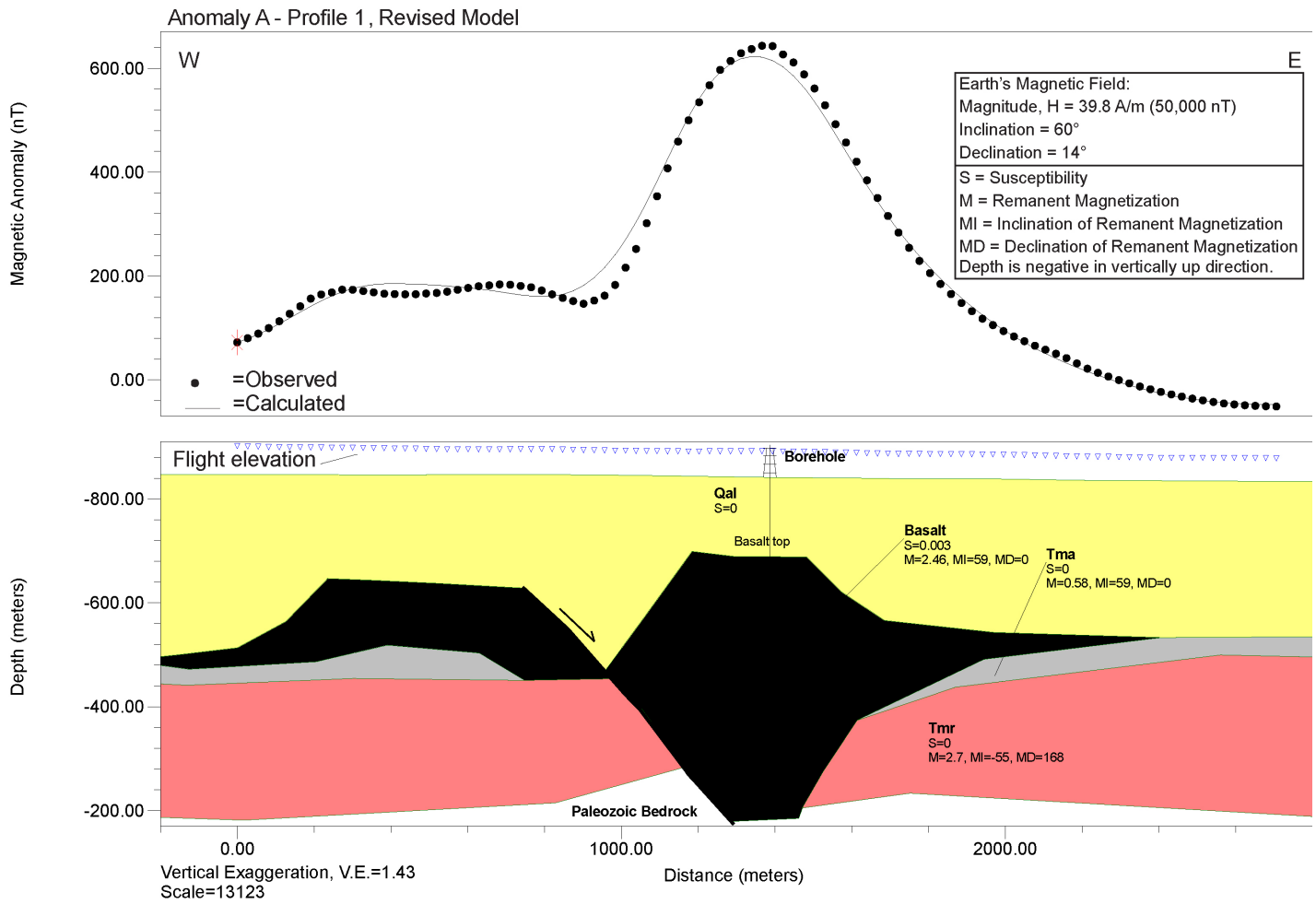

Figure 3-5. Revised Two-Dimensional Model of Anomaly A Along Profile 1 With New Intensity of Basalt. Qal–Quaternary Alluvium, Tma–Ammonia Tanks, Tmr–Rainier Mesa.

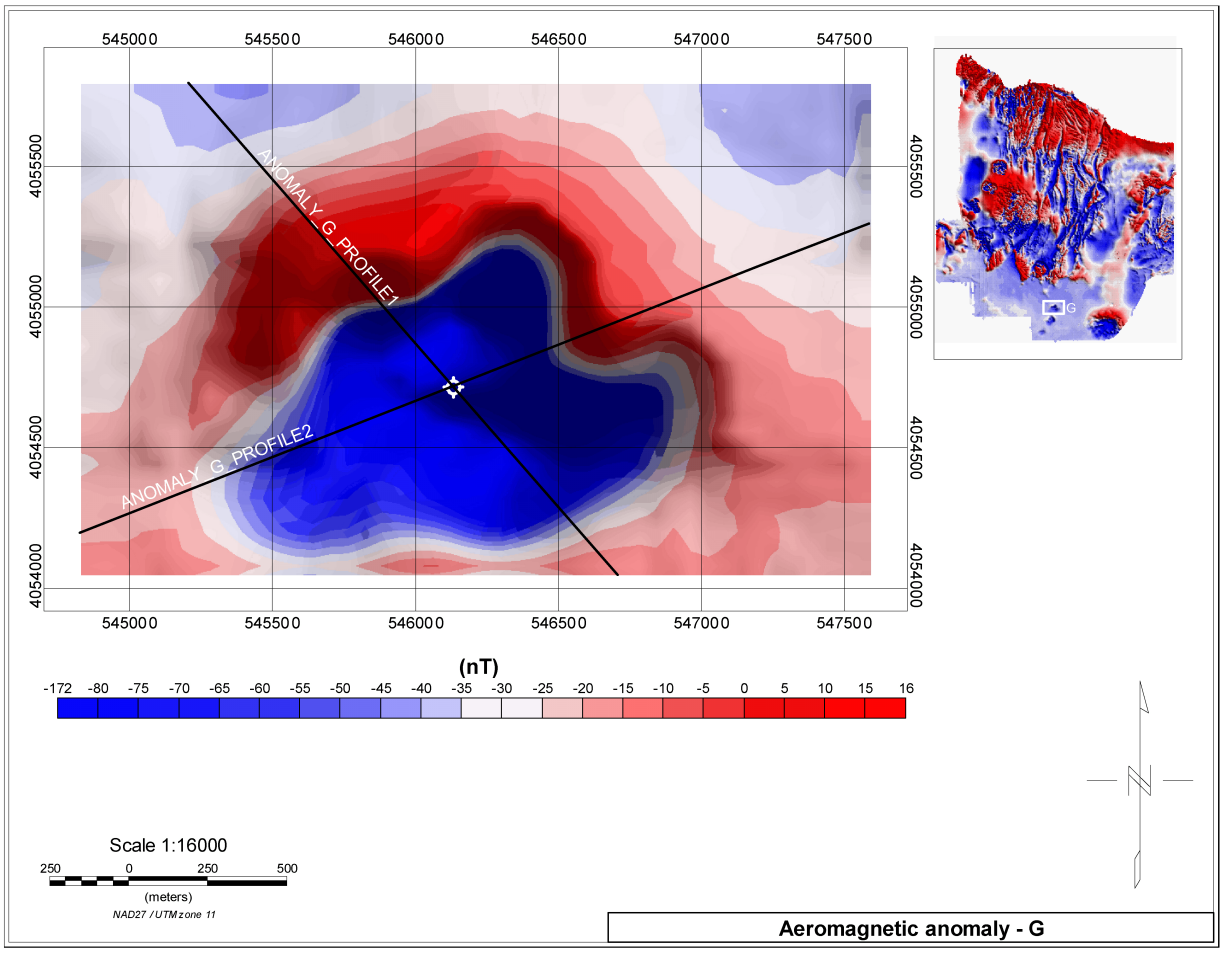

Figure 3-6. Total Field Aeromagnetic Anomaly G Showing Borehole Location and Profile Locations for Two-Dimensional Modeling

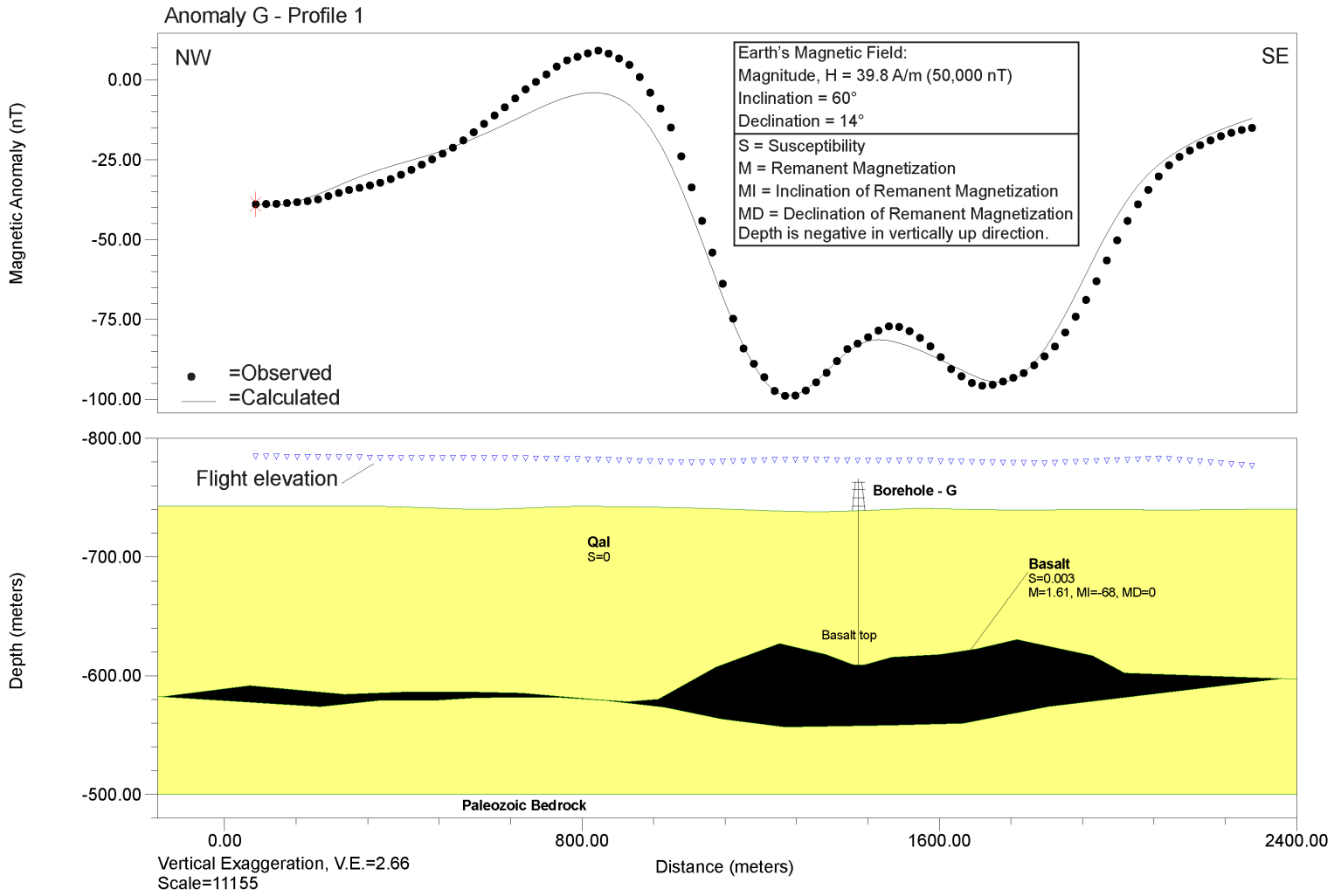

Figure 3-7. Two-Dimensional Model for Anomaly G Along Profile 1. Qal–Quaternary Alluvium.

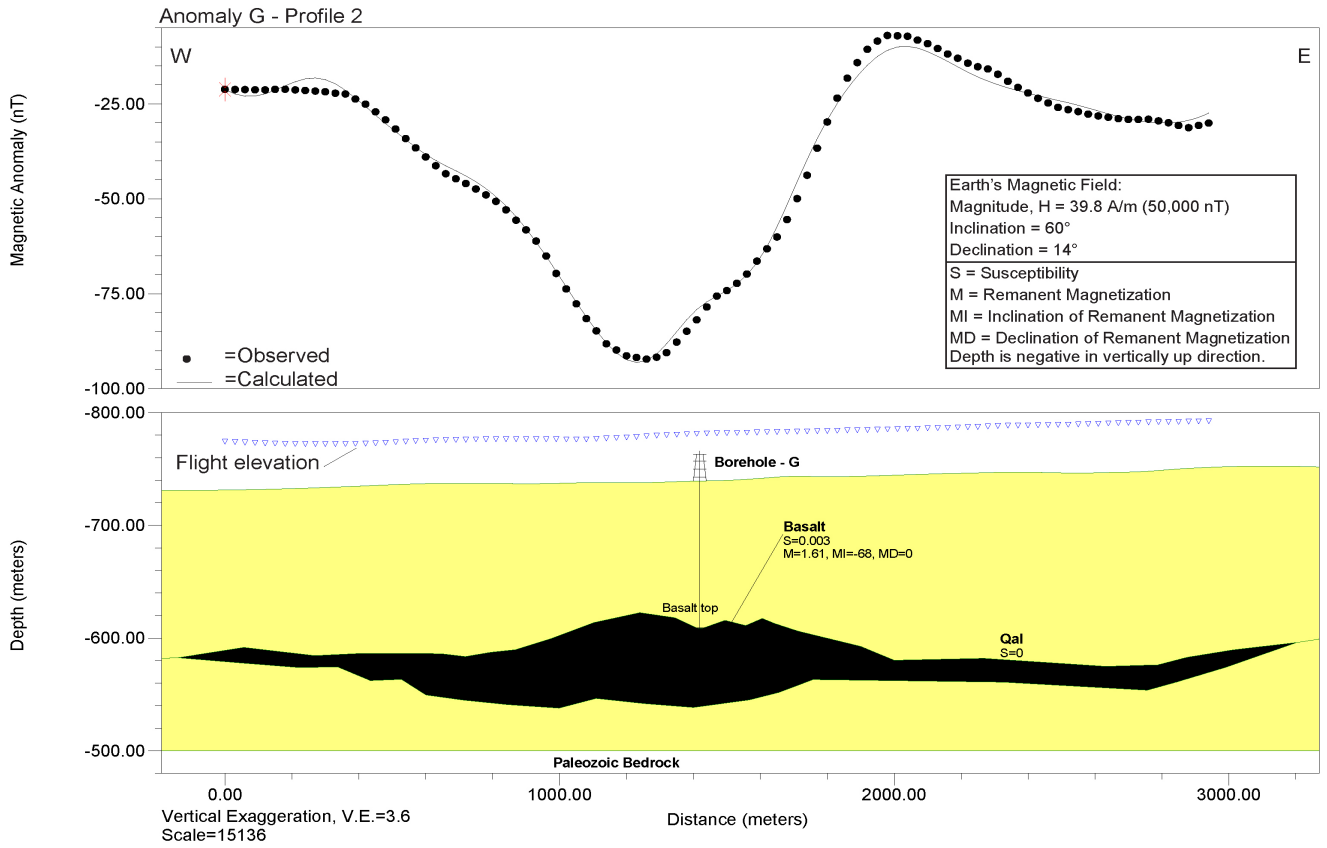

Figure 3-8. Two-Dimensional Model for Anomaly G Along Profile 2. Qal–Quaternary Alluvium.

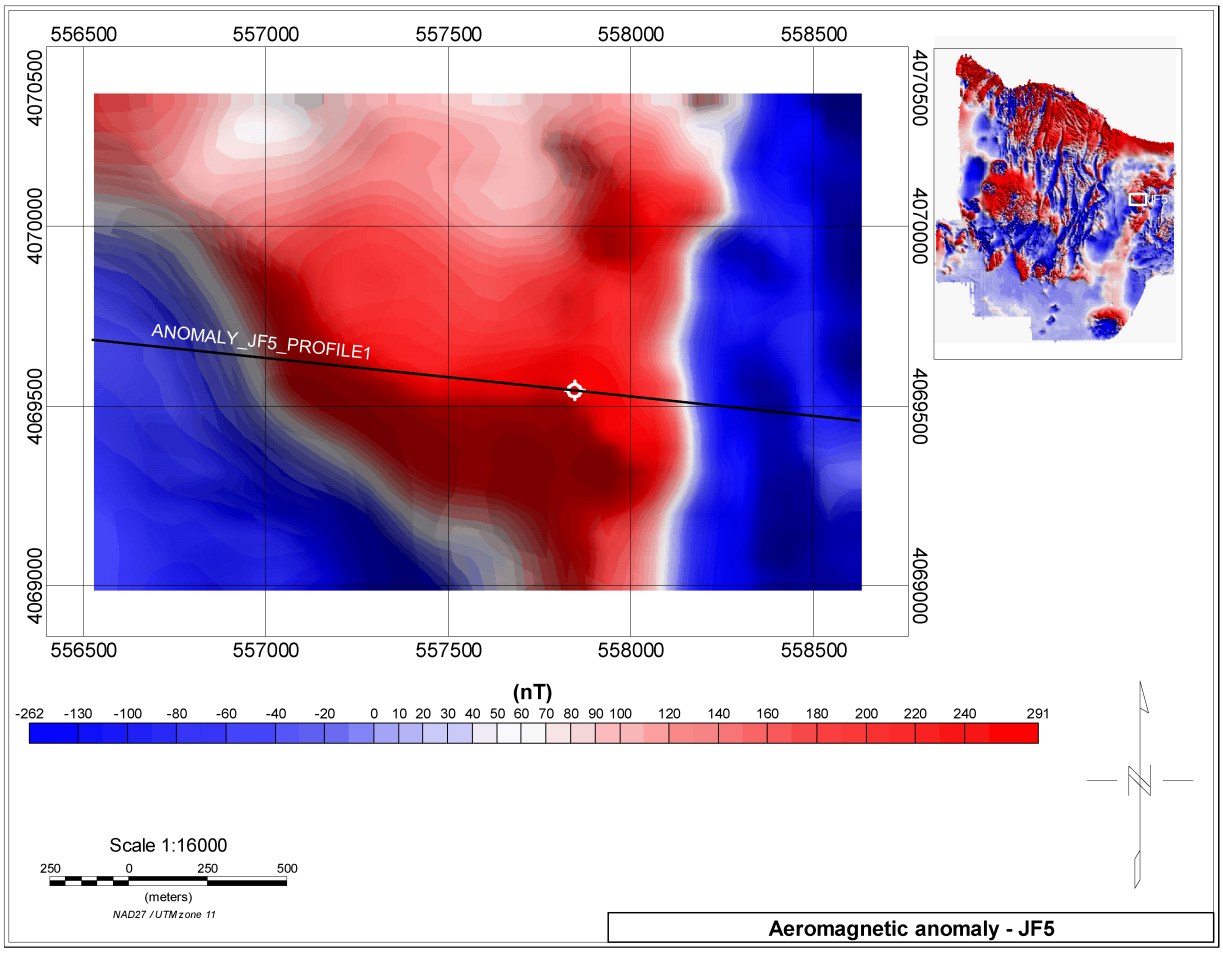

Figure 3-9. Total Field Aeromagnetic Anomaly JF5 Showing Borehole Location and Profile Location for Two-Dimensional Modeling

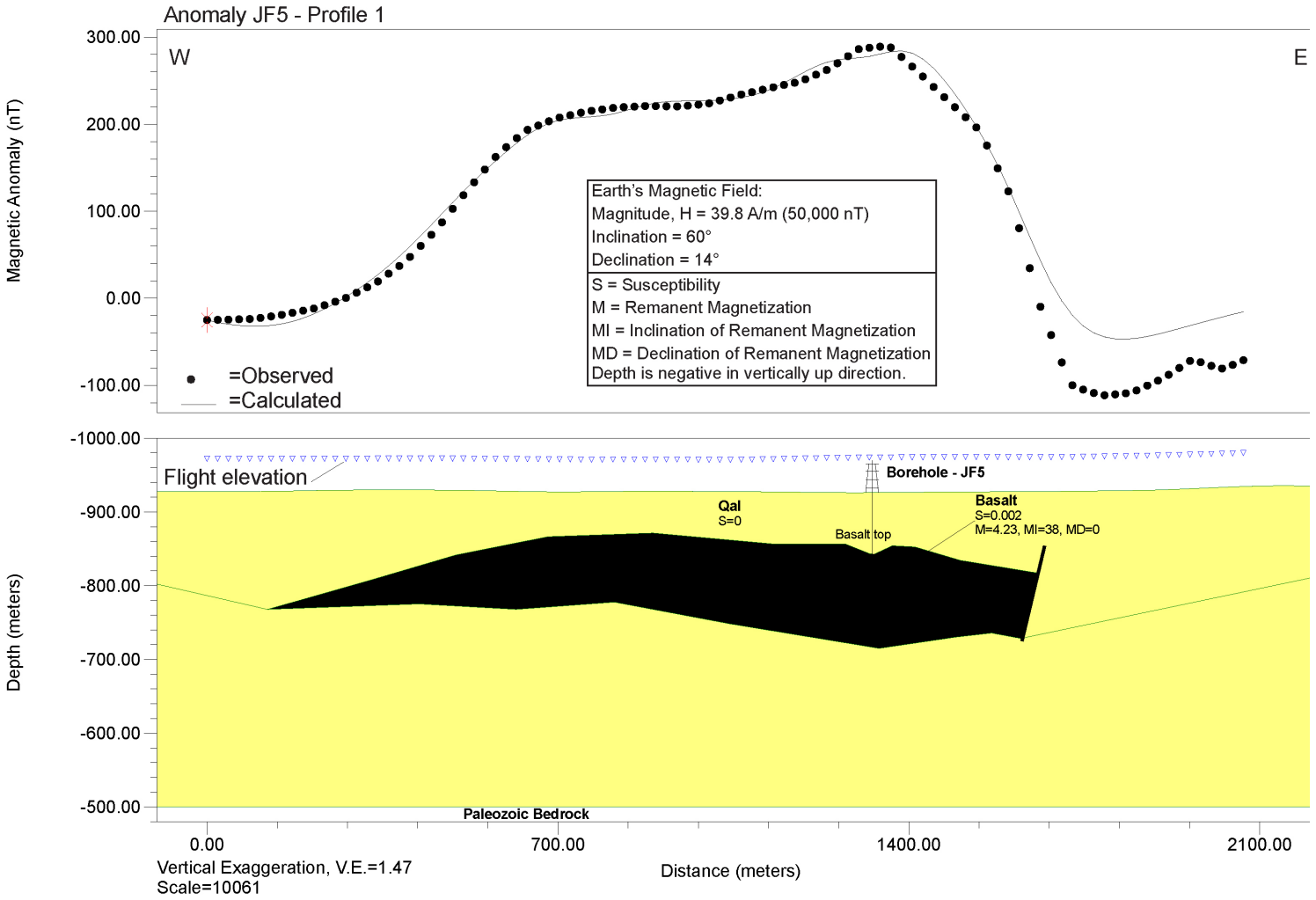

Figure 3-10. Two-Dimensional Model for Anomaly JF5 Along Profile 1. Qal–Quaternary Alluvium.

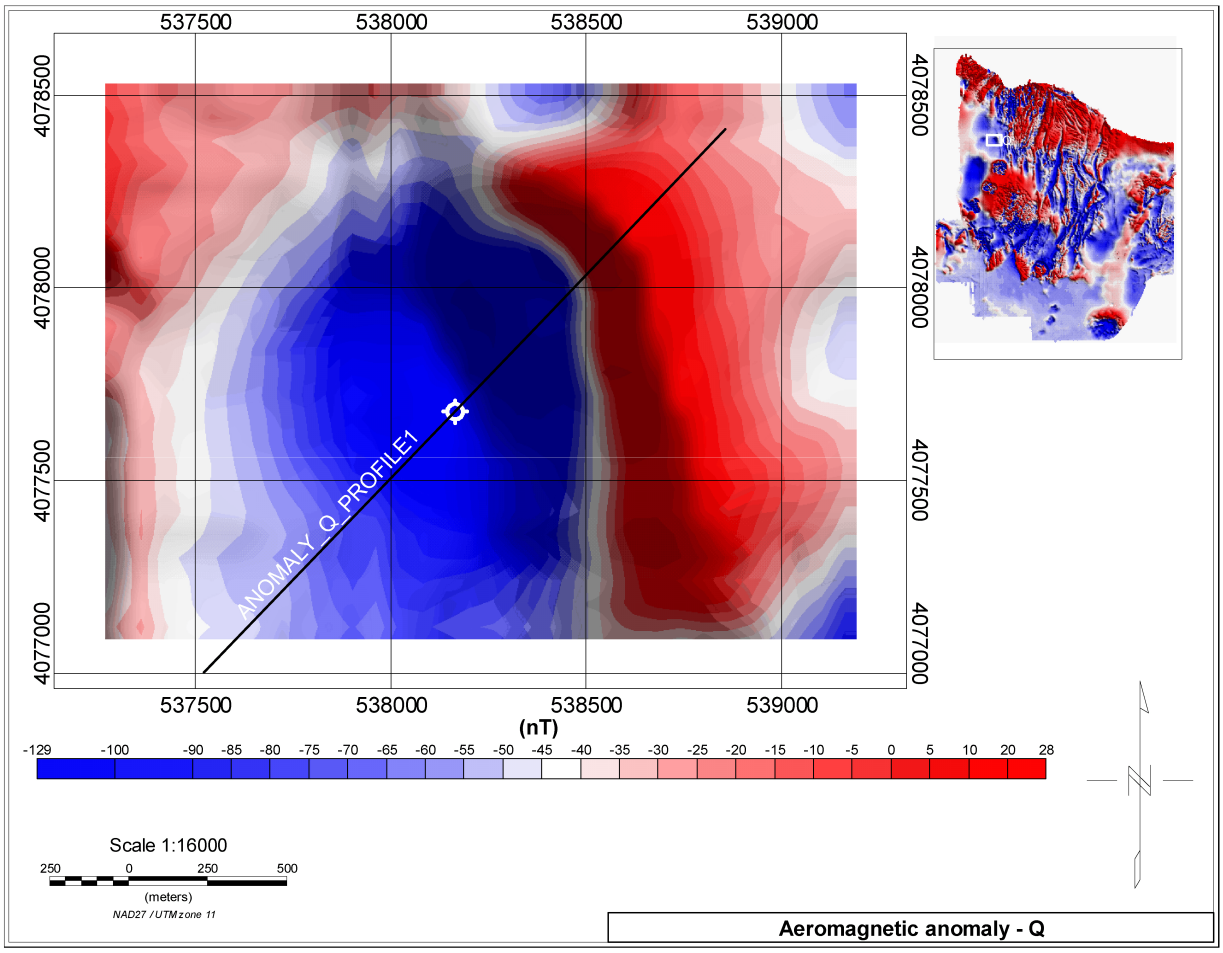

Figure 3-11. Total Field Aeromagnetic Anomaly Q Showing Borehole Location and Profile Location for Two-Dimensional Modeling

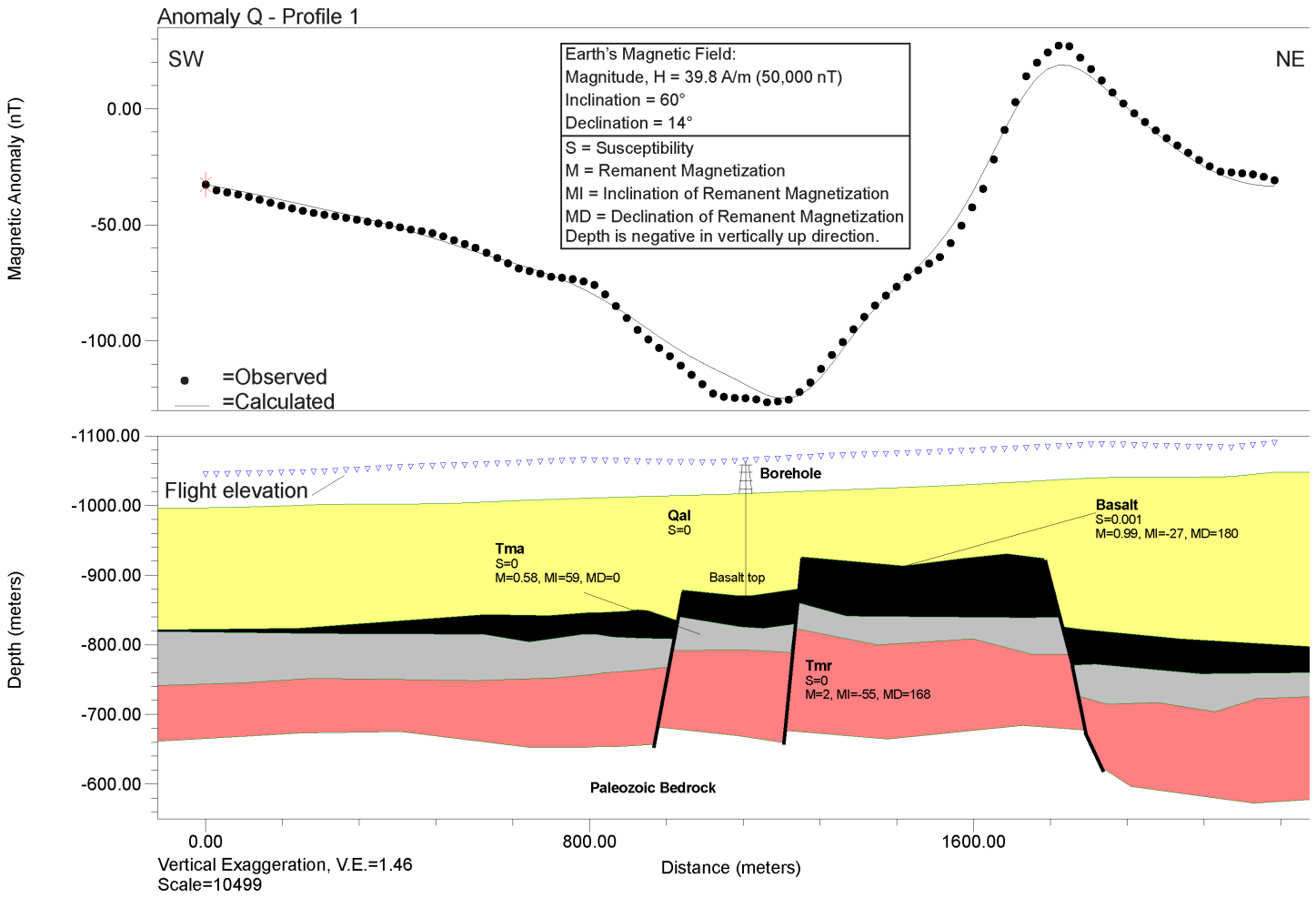

Figure 3-12. Two-Dimensional Model for Anomaly Q Along Profile 1. Qal–Quaternary Alluvium, Tma–Ammonia Tanks, Tmr–Rainier Mesa.

4 ANALYSIS

4.1 Update to Evaluation of Identified Anomalies

In Section 2.4 of Hill and Stamatakos (2002), each of the identified anomalies was described and ranked in terms of a low-medium-high confidence scale with regard to the likelihood that the anomaly represented buried basalt. This section provides an update to the original assessment based on the information obtained since 2002, including the 2004 U.S. Department of Energy (DOE) aeromagnetic data, DOE radiometric age data, and borehole stratigraphy, as well as the petrology, rock magnetic, and paleomagnetic analyses described in Section 2 of this report, coupled with the results of the forward modeling described in Section 3 of this report. Basalt features encountered in the drilling program are ranked as "confirmed" volcanic features. Those features that have been identified as faulted tuff and not basalt have been ranked as "rejected." In Hill and Stamatakos (2002), of the 24 anomalies evaluated, 7 were ranked as "high," 10 as "medium," and 6 as "low." In this update, three anomalies are "rejected," five are confirmed (including anomaly B which was designated as "high" in 2002), six as "high," three as "medium," and nine as "low." This includes the addition of anomalies JF5 and JF6. Table 2-1 of Hill and Stamatakos (2002) has also been updated in this report as Table 4-1 to summarize the new and revised information.

Table 4-1. Revised Summary of Magnetic Anomalies Potentially Representing Buried Basaltic Volcanic Features in the Yucca Mountain Region

Label	Easting	Northing	Polarity	U.S. Geological Survey	Hill and Stamatakos (2002)	This Report	Notes
A	534917	4067499	n	1	high	confirmed	Basanite encountered in borehole at 148 m [486 ft]
B	553787	4051604	r	confirmed	high	confirmed	No change to Hill and Stamatakos (2002)
C	547688	4042829	r	1	high	high	No change to Hill and Stamatakos (2002)
D	549365	4039859	n	1	high	high	No change to Hill and Stamatakos (2002)
E	539038	4047061	n	2	medium	medium	No change to Hill and Stamatakos (2002)
F	545821	4053035	r	1	high	high	Part of F–G–H alignment
G	546132	4054715	r	1	high	confirmed	Basalt encountered in borehole at 119 m [390 ft]
H	544639	4051479	r	1	high	high	Part of F–G–H alignment
I	545154	4057186	n	2	medium	rejected	Tuff encountered in borehole at 163 m [535 ft]
J	540220	4052848	n	3	low	low	No change to Hill and Stamatakos (2002)
K	537980	4042954	n	3	low	low	No change to Hill and Stamatakos (2002)

Table 4-1. Revised Summary of Magnetic Anomalies Potentially Representing Buried Basaltic Volcanic Features in the Yucca Mountain Region (continued)

Label	Easting	Northing	Polarity	U.S. Geological Survey	Hill and Stamatakos (2002)	This Report	Notes
L	531446	4059631	n	3	medium	low	Part of L–M–N–O alignment, faulted tuff
M	532380	4060005	n	3	medium	low	Part of L–M–N–O alignment, faulted tuff
N	533313	4061312	n	3	medium	rejected	Part of L–M–N–O alignment, faulted tuff
O	533779	4062664	n	3	medium	rejected	Tuff encountered in borehole at 163 to 188 m [535 to 617 ft]
P	539474	4076558	r	4	low	low	No change to Hill and Stamatakos (2002)
Q	538167	4077678	r	4	medium	confirmed	Basalt encountered in borehole at 140 to163 m [459 to 535 ft]
R	536985	4079918	r	4	low	high	Part of Q–R alignment or extension of Q flows
S	540407	4082656	r	4	tuff	low	No change to Hill and Stamatakos (2002)
T	535553	4073322	r	?	low	low	No change to Hill and Stamatakos (2002)
1	531735	4065981	r	n/r	medium	medium	No change to Hill and Stamatakos (2002)
2	534189	4063581	r	n/r	medium	low	May be part of L–M–N–O alignment, faulted tuff
3	536916	4055944	n	n/r	medium	medium	No change to Hill and Stamatakos (2002)
4	536520	4077790	n	n/r	low	high	Part of Q–R alignment or extension of Q flows
JF5	557845	4069543	n	n/r	n/r	confirmed	Basalt encountered in borehole at 77 to 94 m [253 to 308 ft]
JF6			n	n/r	n/r	low	Borehole ended in tuff at 196 m [643 ft]

Hill, B.E. and J.A. Stamatakos. "Evaluation of Geophysical Information Used to Detect and Characterize Buried Volcanic Features in the Yucca Mountain Region." San Antonio, Texas: CNWRA. 2002.
Notes: Location coordinates in Universal Transverse Mercator meters, NAD 27, Zone 11; Polarity: n — normal, r — reversed; USGS = Confidence 1–4 from O'Leary, et al. (2002); n/r — not recognized.

- A — Confirmed: Basalt was penetrated by the DOE drill hole at 148 m [486 ft] depth. The average of the two radiometric dates (Table 1-1) suggests it formed 10.6 ± 0.2 million years ago. Paleomagnetic data corroborate the normal-polarity inferred from the anomaly. This age and polarity is consistent with normal-polarity chron C5n.2n (9.920 to

10.494 Ma[1]) of the Geomagnetic Polarity Time Scale (Cande and Kent, 1995). The most likely interpretation of this body is that it is a sill intruded into the surrounding bedrock. Several lines of evidence support this interpretation. First, the feature is exceptionally thick, with a modeled thickness of 500 m [1,640 ft] (Figure 3-5). Considering the thickest exposed lava flows in the area are the 11 Ma flows southeast of anomaly A, which have a maximum thickness on the order of tens of meters, the source for anomaly A appears to be too thick to be a series of stacked lava flows. Second, DOE notes that the core lacks any flow features (Perry, et al., 2006). Third, observations from the thin sections reveal textures, such as biotite pleochroism that are indicative of a slow-cooled intrusive body. This observation of magmatic, as opposed to deuteric biotite (Figure 2-1a), is consistent with the interpretation that anomaly A results from a shallow intrusion.

- B — There is no change to the assessment in Hill and Stamatakos (2002). The anomaly is well south of the DOE helicopter survey (Figure 1-1).

- C–D — There is no change to the assessment in Hill and Stamatakos (2002). These anomalies are south of the DOE helicopter survey (Figure 1-1). In the Blakely (2000) survey, the aeromagnetic signature of C and D appear similar to the anomalies in the F–G–H alignment. As noted in Hill and Stamatakos (2002), basalt was penetrated in the nearby well NCLDC-4a1 at 178 m [584 ft]. Thus, one possibility is that the C–D alignment constitutes volcanoes closely associated to anomaly B and the F–G–H alignment.

- E — There is no change to the assessment in Hill and Stamatakos (2002). The anomaly is well south of the DOE helicopter survey (Figure 1-1).

- G — Confirmed: A basaltic volcanic center was penetrated by a DOE drill hole at 119 m [390 ft] depth. The average of the two radiometric dates (Table 1-1) suggests it formed approximately 3.88 ± .30 million years ago. Paleomagnetic data corroborate reversed-polarity inferred from the anomaly. This age is consistent with the reversed-polarity chron C2Ar (3.580 to 4.180 Ma) of the Geomagnetic Polarity Time Scale (Cande and Kent, 1995). The shape of the anomaly in plan view as well as the shape of the modeled cross-section (Figure 3-8) indicates that this anomaly is the result of a buried cone and associated lava flows. The presence of abundant amphibole ghosts/relicts is unusual and is not reported for anomaly B or other Pliocene lavas in the Yucca Mountain region.

- F and H — Similar aeromagnetic anomaly signature to anomaly G. In addition, the alignment of G, F, and H indicate that F and H are part of the same volcanic system as the buried volcano that produces the anomaly at G. Thus, there is high confidence in the interpretation of buried basalt. Anomalies F and H are also interpreted as equivalent in age to the dated basalt at anomaly G based to characteristic size and alignment (cf. 1 Ma and 3.8 Ma Crater Flat alignments, Figure 1-1).

- I — Rejected: Tuff was encountered at 163 m [535 ft], and the borehole ended in tuff at a depth of 200 m [656 ft] in tuff.

[1]Ma is a geological acronym meaning “million of years before present” that is used frequently in this report.

- J — There is no change to the assessment in Hill and Stamatakos (2002). The anomaly is just south of the DOE helicopter survey (Figure 1-1).

- K — There is no change to the assessment in Hill and Stamatakos (2002). The anomaly is well south of the DOE helicopter survey (Figure 1-1).

- L–O — Rejected: Tuff was encountered in the borehole at depths between 163 and 188 m [535 and 617 ft].

- P — There is no change to the assessment in Hill and Stamatakos (2002). Consistent with the interpretation in Hill and Stamatakos (2002), the 2004 aeromagentic map from the DOE helicopter survey shows that this anomaly most likely represents the southern extent of a generally north-trending buried scarp of faulted tuff.

- Q — Confirmed: Basalt was penetrated by the DOE drill hole at depths between 140 and 163 m [459 and 535 ft]. The two radiometric dates (Table 1-1) suggest the basalt was erupted approximately 10.94 ± 0.5 million years ago. The drill core revealed four individual lava flows, each separated by scoria and breccia. Paleomagnetic data corroborate that the upper flow has a reversed-polarity magnetization, as inferred from the anomaly. This age is consistent with the reversed-polarity chron C5r.1r (10.94–11.05 Ma) of the Geomagnetic Polarity Time Scale (Cande and Kent, 1995). Lower flows may have a normal-polarity magnetization, although the paleomagnetic signal recovered from these lower flows is of poor quality. Forward modeling suggest that the flows are part of an extensive area of highly faulted lava within Crater Flat basin. The flows are very similar to the basalt flows that crop out in the low hills south of Crater Flat and in borehole USW-VH2. Similarities include the radiometric ages, stratigraphic position beneath megabreccia landslide deposits, and nature of the basalt.

- R — High Confidence: This isolated anomaly with reversed-polarity magnetization projects along a possible northwest-trending alignment with anomaly Q. Based on the similarities in the expression anomaly, it appears that this anomaly also results from the 11 Ma basalt observed in the drill hole at anomaly Q.

- S — There is no change to the assessment in Hill and Stamatakos (2002).

- T — There is no change to the assessment in Hill and Stamatakos (2002).

- 1 — There is no change to the assessment in Hill and Stamatakos (2002). However, the large amplitude of this anomaly, its normal polarity, and its proximity to anomaly A suggest that it may be related to the basalt discovered at anomaly A.

- 2 — Low Confidence: This anomaly is similar in character and closely associated with anomaly O. The drill hole at anomaly O encountered tuff, not basalt.

- 3 — There is no change to the assessment in Hill and Stamatakos (2002).

- 4 — High Confidence: This isolated anomaly with reversed-polarity magnetization projects along a possible northwest-trending alignment with anomaly Q. Based on the

similarities in the expression anomaly, it appears that this anomaly also results from the 11 Ma basalt observed in the drill hole at anomaly Q.

- JF5 — Confirmed: Basalt was penetrated by the DOE drill hole at depths between 77 and 94 m [253 and 308 ft]. The radiometric date (Table 1-1) suggests the basalt was erupted approximately 9.4 ± 0.2 million years ago. Paleomagnetic data corroborate that the basalt has a normal-polarity magnetization, as inferred from the anomaly. However, this age is not consistent with the Geomagnetic Polarity Time Scale (Cande and Kent, 1995). Reversed-polarity chron C4Ar.2r spans the interval between 9.308 and 9.580 Ma. The paleomagnetic data among each of the three core samples are sufficiently dissimilar to suggest that the cored basalts may have recorded progressive horizontal-axis rotation of the flows due to faulting. Given the uncertainty range, the age of this basalt could be as young as 9.2 Ma, corresponding to normal Chron C4Ar.1n, or as old as 9.6 Ma, corresponding to normal C4Ar.2n. Anomaly JF6 is located about 3 km [1.9 mi] from JF5 in the southwest direction. No basalt was observed in the JF6 borehole.

4.2 Update to Potential Effects on Probability Models

In Hill and Stamatakos (2002), at least 10 anomalies were ranked as having medium to high confidence that they were caused by buried basaltic volcanoes. These 10 sources were not evaluated as part of the original DOE PVHA (CRWMS M&O, 1996). These 10 anomalies (H, I, L, M, N, O, Q, 1, 2, and 3) could be interpreted to represent 10 individual buried volcanic centers or 6 to 8 events of aligned volcanoes. The 10 volcanoes essentially doubled the number of events the experts considered in the 1996 PVHA. Based on that assessment, Hill and Stamatakos (2002) proposed three hypotheses on how these additional features could affect the DOE probability models:

(1) There would be no effect on the models if all the buried volcanoes were older than about 5 Ma because the DOE experts in the original expert elicitation did not consider any events older than 5 Ma.

(2) Uniform recurrence rate experts considered in the original DOE expert elicitation would double. This factor of two increase arises because the DOE experts generally considered an average recurrence rate of about one to three volcanoes per million years over the interval between 2 and 5 Ma. Adding 10 events leads to a uniform recurrence rate of 2 to 6 volcanoes per million years.

(3) There could potentially be up to an order of magnitude increase in probability if the 10 volcanoes formed within a single episode of intense volcanism in the Pliocene,[2] about 4 million years ago, and this episodic rate is applicable to Yucca Mountain over the compliance period. Adding the 10 volcanic events to the 4 to 10 recognized Pliocene events thereby increases the average recurrence rate for that interval to 14–20 volcanoes per million years.

[2]The Pliocene is the epoch of geologic time between 5.3 to 1.8 Ma.

Of those 10 anomalies, 4 (L, M, N, and 2) are reinterpreted as having low confidence that they are caused by a buried basaltic volcanic feature, and 2 (I and O) have been "rejected" because the DOE drilling encountered tuff, not basalt (Table 4-1). One, anomaly Q, was "confirmed" based on the DOE drilling. Three (H, 1, and 3) remain ranked as anomalies that have a medium to high confidence of being a buried basaltic volcano. In addition, the DOE encountered basalt at JF5, which was not an anomaly evaluated in Hill and Stamatakos (2002).

Thus, based on these volcano counts alone, the results of the new data can be used to assess these three hypotheses.

(1) There is no change to this hypothesis, because only one (anomaly H) of the 10 not considered in the original 1996 DOE PVHA can be shown to be a volcanic feature younger than 5 Ma. Anomaly H is part of the F–G–H alignment in which Pliocene basalt was encountered by drilling at anomaly G.

(2) This hypothesis now seems unlikely. There is no evidence from the new information to add more than one volcano with an age between 2 and 5 Ma to the original DOE count in the PVHA (CRWMS M&O, 1996).

(3) Although the new data do not support adding 10 volcanoes to the Pliocene cluster as proposed by this hypothesis, the new data, especially the new age dates from the basalt recovered from the drill holes at A, G, JF5, and Q, strongly support the interpretation that past volcanism of Yucca Mountain occurred in temporal clusters. At least three clusters can be recognized from the volcanic record (Table 4-2).

While the new information reduced the number of possible events in the cluster compared to what was proposed in hypothesis (3) of Hill and Stamatakos (2002), the new age data also reduced uncertainty in the time spanned by the temporal Pliocene cluster. Thus, an episodic recurrence rate of 10 or more volcanoes per million years still warrants consideration.

Another implication to DOE probability models that may need additional assessment is the possibility that anomaly A represents a basaltic intrusion or sill. The presence of a sill beneath Crater Flat was proposed by Brocher, et al. (1998) and our interpretation of anomaly A is consistent with this hypothesis. Current DOE and Center for Nuclear Waste Regulatory Analyses probability models are focused on the likelihood of a volcanic dike intersecting one or several drifts in the potential repository and the associated likelihood that the dike will break through the surface to form a volcanic cone. Although the likelihood of sill formation, given that an igneous event occurs, cannot be reliably estimated at this time, current interpretations indicate that this process may be a credible natural event in the Yucca Mountain region.

Table 4-2. Temporal Clusters of Past Volcanism in the Yucca Mountain Region

Temporal Cluster	Events*	Number of Events	Recurrence Rate
Quaternary† 0.08–1 Ma‡	NE Little Cone SW Little Cone Red Cone Black Cone Northern Cone Hidden Cone Little Black Peak Lathrop Wells	8	8 volcanoes per million years
Pliocene§ 3.6–4.7 Ma	3–6 vents in Crater Flat Anomalies F, G, and H Anomaly B 3–5 vents at Thirsty Mesa Anomalies C and D‖	12–17	11–16 volcanoes per million years
Miocene# 9.0-11.2 Ma	Anomaly A Solitario Canyon Dike JF5 and Fortymile Wash Crater Flat**	Unknown	Insufficient information to resolve the number of vents for Crater Flat basalt and nature of Anomaly A

*Identified volcanic events as defined in CRWMS M&O (1998)††, Hill and Stamatakos (2002)‡‡, or Connor and Connor (2007)§§.
†The Quaternary is the subdivision of geologic time between 1.8 Ma and the present.
‡Ma is million of years before present.
§The Pliocene is the epoch of geologic time from 1.8 to 5.3 Ma.
‖Based on similar character and burial depth to F–G–H alignment and anomaly B.
#The Miocene is the epoch of geologic time from 5.3 to 23.2 Ma.
**Includes all 11.1–11.2 Ma basalt in Crater Flat, including the basalt in USW-VH2, anomaly Q drill hole, and the exposure in the low hills south of Crater Flat.
††CRWMS M&O. "Synthesis of Volcanism Studies for the Yucca Mountain Site Characterization Project." F.V. Perry, B.M. Crowe, G.A. Valentine, and L.M. Bowker, eds. MOL.19980722.0048. Las Vegas, Nevada: DOE, Office of Civilian Radioactive Waste Managerment. 1998.
‡‡Hill, B.E. and J.A. Stamatakos. "Evaluation of Geophysical Information Used to Detect and Characterize Buried Volcanic Features in the Yucca Mountain Region." San Antonio, Texas: CNWRA. 2002.
§§Connor, C. and L. Connor. "Probabilistic Assessments of Volcanic Hazards at Yucca Mountain, NV." Transcript of 176th Advisory Committee on Nuclear Waste Meeting, Rockville, Maryland, February 13, 2007. ML070580160. pp. 1–203. Rockville, Maryland: NRC. 2007.

5 SUMMARY AND CONCLUSIONS

The U.S. Department of Energy (DOE)-sponsored helicopter aeromagnetic survey of the Yucca Mountain region is the most detailed regional magnetic anomaly map to date and provides an improved tool for the interpretation of buried or shallowly intruded basaltic features. More importantly, the DOE drilling program completed seven drill holes at selected anomaly sites in Crater Flat, Jackass Flat, and the Amargosa Desert. Basalt was recovered from four of the drill holes at depths between 80 and 150 m [262 and 492 ft]. Cores of the basalt were recovered, and radiometric ages for the basalt samples were obtained by DOE. The ages show that the basalt at anomalies A, JF5, and Q are between 9.4 ± 0.2 and 11.7 ± 0.2 Ma. Basalt recovered from the drill hole at anomaly G was dated at 3.74 ± 0.21 and 3.99 ± 0.22 Ma.

Two-dimensional magnetic anomaly models of the four anomalies from buried basalt were developed to interpret the shape and nature of the source bodies. Magnetic parameters used to characterize the magnetic sources were obtained from rock magnetic and paleomagnetic analyses performed on subsamples of the four basalt cores. Results show that the magnetization of the basalts is dominated by a thermo-remanent magnetization carried by pseudosingle domain magnetite that appears to preserve a record of Earth's magnetic field at the time the basalts formed, including reversals of Earth's magnetic field. Samples from cores at anomalies A and JF5 have normal polarity directions, while those from G and the upper flows at Q carry reversed polarity directions. Demagnetization of the lower flows in the core at anomaly Q are poor but suggest that a reversal of the field may be preserved in these samples. Polarity of the samples agrees with corresponding ages of the normal or reversed chrons of the geomagnetic polarity time scale except for the samples at JF5. Additional analysis of the radiometric data may be necessary to further establish the age of these flows in Jackass Flat.

Based on the magnetic modeling and DOE age data, the relative ranking of the anomalies with regard to the likelihood that they are produced by buried basaltic volcanic features developed in Hill and Stamatakos (2002) was updated. Of the 10 anomalies originally ranked as medium to high, only 3 remain uncertain. The others were either rejected because the DOE drilling intersected tuff, not basalt, or were downgraded to a ranking of low because they were similar to features that are known to be tuff. DOE also encountered basalt at JF5, which was not one of the ranked anomalies. Thus, the new information has reduced uncertainty in the number of past igneous events at Yucca Mountain. However, a possibility for present, but still undetected, basalts cannot be dismissed.

The new age data also reduced the uncertainty in timing of past episodes of volcanism at Yucca Mountain. Three clusters of past activity can be recognized from the data: one between about 9 and 11.2 Ma, one between 3.6 and 4.7 Ma, and one between 80,000 years and 1 Ma. Of these, the cluster between 3.6 and 4.7 Ma is significant because it includes a relatively large number of volcanic events that led to an episodic recurrence rate substantially greater than long-term averages for Yucca Mountain. These data suggest that temporal clustering is an important characteristic of the Yucca Mountain volcanic system that may warrant consideration in volcanic hazard probability models.

A second important conclusion of the new data comes from the analysis of core at anomaly A. Magnetic modeling coupled with observations from the core and from thin sections suggest that this basalt is a relatively thick intrusion or sill of basalt. Confirmation that this body is a sill is important because sill formation may be accompanied by large increases in thermal gradient

and changes in rock stress patterns for rocks overlying the sill. The magnitude and extent of the potential effects of sill formation may warrant future consideration.

Finally, it is important to note that the observation of amphibole in basalt from the core at anomaly G suggests that the Pliocene basalt melt was also erupted at near water saturated conditions. The Pliocene magma shares these characteristics with similar observations from the Quaternary hawaiite erupted in Crater Flat.

6 REFERENCES

Blakely, R.J., V.E. Langenheim, D.A. Ponce, and G.L. Dixon. "Aeromagnetic Survey of the Amargosa Desert, Nevada and California: A Tool for Understanding Near-Surface Geology and Hydrology." U.S. Geological Survey Open-File Report 00-1 88. 2000.

Brocher, T.M., W.C. Hunter, and V.E. Langenheim. "Implications of Seismic Reflection and Potential Field Geophysical Data on the Structural Framework of the Yucca Mountain—Crater Flat Region, Nevada." *Geological Society of America Bulletin*. Vol. 110. pp. 947–971. 1998.

Cande, S.C. and D.V. Kent. "Revised Calibration of the Geomagnetic Polarity Time Scale for the Late Cretaceous and Cenozoic." *Journal of Geophysical Research*. Vol. 100. pp. 6,093–6,095. 1995.

Connor, C. and L. Connor. "Probabilistic Assessments of Volcanic Hazards at Yucca Mountain, NV." Transcript of 176th Advisory Committee on Nuclear Waste Meeting, Rockville, Maryland, February 13, 2007. ML070580160. pp. 1–203. 2007.

Connor, C.B., J.A. Stamatakos, D.A. Ferrill, B.E. Hill, G. Ofoegbu, F.M. Conway, B. Sagar, and J.S. Trapp. "Geologic Factors Controlling Patterns of Small-Volume Basaltic Volcanism: Application to a Volcanic Hazards Assessment at Yucca Mountain, Nevada." *Journal of Geophysical Research*. Vol. 105. pp. 417–432. 2000.

Connor, C.B., S. Lane-Magsino, J.A. Stamatakos, R.H. Martin, P.C. LaFemina, B.E. Hill, and S. Lieber. "Magnetic Surveys Help Reassess Volcanic Hazards at Yucca Mountain, Nevada." *EOS, Transactions of the American Geophysical Union*. Vol. 78, No. 7. pp. 73–78. 1997.

Coppersmith, K.J., K. Jenni, T. Nieman, R. Perman, R. Youngs, F. Perry, and M. Cline. "Update to the Probabilistic Volcanic Hazard Analysis, Yucca Mountain, Nevada." Proceedings of American Geophysical Union Fall Meeting, San Francisco, California, December 5–9, 2005. Abstract No. V31E-07. 2005.

CRWMS M&O. "Characterize Framework for Igneous Activity at Yucca Mountain, Nevada." ANL–MGR–GS–000001. Rev. 00, ICN 01. North Las Vegas, Nevada: DOE, Yucca Mountain Site Characterization Office. 2000a.

———. "Total System Performance Assessment for the Site Recommendation." TDR–WIS–PA–000001. Rev. 00, ICN 01. North Las Vegas, Nevada: DOE, Yucca Mountain Site Characterization Office. 2000b.

———. "Synthesis of Volcanism Studies for the Yucca Mountain Site Characterization Project." F.V. Perry, B.M. Crowe, G.A. Valentine, and L.M. Bowker, eds. MOL.19980722.0048. Las Vegas, Nevada: DOE, Office of Civilian Radioactive Waste Management. 1998.

———. "Probabilistic Volcanic Hazards Analysis for Yucca Mountain, Nevada." BA0000000–1717–2200–00082. Rev. 00. North Las Vegas, Nevada: DOE, Yucca Mountain Site Characterization Office. 1996.

Day, R., M.D. Fuller, and V.A. Schmidt. "Hysteresis Properties of Titanomagnetites: Grain Size and Composition Dependence." *Physics of the Earth and Planetary Interiors*. Vol. 13. pp. 260–266. 1977.

Dunlop, D.J. and Ö. Özdemir. *Rock Magnetism: Fundamentals and Frontiers*. Cambridge, United Kingdom: Cambridge University Press. 1997.

Electric Power Research Institute. "Igneous Event Scenario." Palo Alto, California: Electric Power Research Institute. 2003.

Evans, M.E. and F. Heller. *Environmental Magnetism: Principles and Applications of Environmagnetics*. Amsterdam, Netherlands: Academic Press, Elsevier Science. 2003.

Fleck, R.J., B.D. Turrin, D.A. Sawyer, R.G. Warren, D.E. Champion, M.R. Hudson, and S.A. Minor. "Age and Character of Basaltic Rocks of the Yucca Mountain Region, Southern Nevada." *Journal of Geophysical Research*. Vol. 101. pp. 8,205–8,227. 1996.

Fridrich, C.J. "Tectonic Evolution of the Crater Flat Basin, Yucca Mountain Region, Nevada, Cenozoic Basins of the Death Valley Region." *Cenozoic Basins of the Death Valley Region*. L.A. Wright and B.W. Troxel, eds. Geological Society of America Special Paper 333. pp. 169–196. 1999.

Geosoft, Inc. "Oasis MONTAJ™." Version 6.3.1 (6G). Toronto, Ontario, Canada: Geosoft, Inc. 2006.

Hagstrum, J.T., M.G. Sawlan, B.P. Hausback, J.G. Smith, C.S. Grommé. "Miocene Paleomagnetism and Tectonic Setting of the Baja California Peninsula, Mexico." *Journal of Geophysical Research*. Vol. 92. pp. 2,627–2,640. 1987.

Hill, B.E. and J.A. Stamatakos. "Evaluation of Geophysical Information Used to Detect and Characterize Buried Volcanic Features in the Yucca Mountain Region." San Antonio, Texas: CNWRA. 2002.

Ho, C.-H. and E.I. Smith. "A Spatial-TemporaV3-D Model for Volcanic Hazard Assessment: Application to the Yucca Mountain Region, Nevada." *Mathematical Geology*. Vol. 30, No. 5. pp. 497–510. 1998.

Kirschvink, J.L. "The Least Squares Lines and Planes and the Analysis of Paleomagnetic Data." *Geophysical Journal of the Royal Astronomical Society*. Vol. 62. pp. 699–718. 1980.

Langenheim, V.E. "Magnetic and Gravity Studies of Buried Volcanic Centers in the Amargosa Desert and Crater Flat, Southwest Nevada." U.S. Geological Survey Open-File Report 95-564. 1995.

Magsino, S.L., C.B. Connor, B.E. Hill, J.A. Stamatakos, P.C. La Femina, D.A. Sims, and R.H. Martin. "CNWRA Ground Magnetic Surveys in the Yucca Mountain Region, Nevada (1996–1997)." CNWRA 98–001. San Antonio, Texas: CNWRA. 1998.

McFadden, P.L. and A. Reid. "Analysis of Paleomagnetic Inclination Data." *Geophysical Journal of the Royal Astronomical Society*. Vol. 69. pp. 307–319. 1982.

Nicholis, M.G. and M.J. Rutherford. "Experimental Constraints on Magma Ascent Rate for the Crater Flat Volcanic Zone Hawaiite." *Geology*. Vol. 32. pp. 489–492. 2004.

Northwest Geophysical Association. "GM-SYS©." Version 4.8.45b. Corvallis, Oregon: Northwest Geophysical Association. 2001.

NRC. NUREG-1762, "Integrated Issue Resolution Status Report." Vol. 2. Rev. 2. Washington, DC: NRC. 2005.

———. NUREG–1804, "Yucca Mountain Review Plan—Final Report." Rev. 2. Washington, DC: NRC. July 2003.

O'Leary, D.W., E.A. Mankinen, R.J. Blakely, V.E. Langenheim, and D.A. Ponce. "Aeromagnetic Expression of Buried Basaltic Volcanoes Near Yucca Mountain, Nevada." U.S. Geological Survey Open-File Report 02-020. 2002.

Perry, F., A. Cogbill, R. Kelly, M. Cline, C. Lewis, and R. Fleck. "Status and Interpretation of Aeromagnetic Survey and Drilling Program to Support Probabilistic Volcanic Hazard Analysis–Update." Transcripts of the 172nd Advisory Committee on Nuclear Waste Meeting, Rockville, Maryland, July 17, 2006. ML062090096. pp. 1–164. 2006.

Perry, F.V., A. Cogbill, R. Kelley, R. Youngs, and M. Cline. "Updating an Expert Elicitation in Light of New Data: Ten Years of Probabilistic Volcanic Hazard Analysis for the Proposed High-Level Radioactive Waste Repository at Yucca Mountain, Nevada." *EOS, Transactions*. American Geophysical Union. Vol. 82. 2005.

Potter, C.J., R.P. Dickerson, D.S. Sweetkind, R.M. Drake II, E.M. Taylor, C.J. Fridrich, C.A. San Juan, and W.C. Day. "Geologic Map of the Yucca Mountain Region, Nye County, Nevada." U.S. Geological Survey Geologic Investigations Series Map I-2755. Scale 1:50,000. 2002.

Rosenbaum, J.G. and D.B. Snyder. "Preliminary Interpretation of Paleomagnetic and Magnetic Property Data From Drill Holes USW G-1, G-2, G-3, and VH-1 and Surface Localities in the Vicinity of Yucca Mountain, Nye County, Nevada." U.S. Geological Survey Open-File Report 85-49. 1985.

Schlueter, J.R. "Request for Additional Information—Igneous Activity Agreement 1.02." Letter (December 19) to J.D. Ziegler, DOE. Washington, DC: NRC. 2002.

Stamatakos, J.A., C.B. Connor, and R.H. Martin. "Quaternary Basin Evolution and Basaltic Volcanism of Crater Flat, Nevada, From Detailed Ground Magnetic Surveys of the Little Cones." *Journal of Geology*. Vol. 105. pp. 319–330. 1997.

Valentine, G.A. and K.E.C. Krogh. "Emplacement of Shallow Dikes and Sills Beneath a Small Basaltic Volcanic Center—The Role of Pre-Existing Structures (Paiute Ridge, Southern Nevada, USA)." *Earth and Planetary Science Letters*. Vol. 246. pp. 217–230. 2006.

Vaniman, D.T., B.M. Crowe, and E.S. Gladney. "Petrology and Geochemistry of Hawaiite Lavas From Crater Flat, Nevada." *Contributions to Mineralogy and Petrology*. Vol. 80. pp. 341–357. 1982.

Ziegler, J.D. "Igneous Activity Agreement (IA) 1.02 Additional Information Needed (AIN-1): U.S. Department of Energy (DOE) Position on Volcanic Hazard at Yucca Mountain, Nevada, and Plans for Confirmatory Studies." Letter (November 5) to J.R. Schlueter, NRC. Las Vegas, Nevada: DOE. 2003. <www.nrc.gov/reading-rm/adams.html> (March 2007).